Comparative study of spark channel expansion in water

V. Stelmashuk, P. Hoffer, K. Koláček, J. Štraus

Institute of Plasma Physics of the CAS, Prague, Czech Republic

Abstract: Expansion of plasma liquid interface of spark discharge produced in water was studied from the point of view of energy conversion. The spark expansion was observed by means of high speed imaging, and the electric power dissipated in the spark was measured. Different mathematical models of spark expansion (Naugolnych and Roy, Braginskii, and Engel) were used for theoretical calculation of the spark expansion at a given input power. Results are compared to the measured data.

Keywords: spark discharge, water, plasma channel, modeling

1. Introduction

The generation of shock waves in water by electrical discharge finds various industrial implementations, including medical applications [1], oil gas technology for well stimulation [2], electrical discharge machining [4, 5]. Along with these numerous accomplishments, the mathematical description of a spark channel expansion in water requires further development and its refinement. The main difficulty in verification of numerous mathematical models is a lack of experimental studies observing spark channel expansion just after electrical breakdown, when the shock wave is formed. As a rule, the authors compare an acoustical signature produced by the underwater discharge or/and how the modeled bubble cavitation period matches with the experiment [5−9]. Author found a single publication reporting an accurate modeling of pulsed spark discharge in water and its comparison with experiment [10]. The presented investigation does not pretend to offer a novel mathematical approach to the problem, but rather to evaluate the existing models in uncompressible approximation and compare them with the experimental results.

2. Experimental setup

Electrical underwater discharge was generated by discharging a capacitor bank via an electrode system mounted in a laboratory tank filled with tap water (Fig. 1). The spark was generated between two electrodes made of tungsten wires with diameter of 0.8 mm. The electrode gap was between 0.75–0.8 mm. The capacitor bank C_s (0.8 µF) charged to 12 kV-30 kV was used as a source of energy. The gas filled spark gap was used as a switch. Video sequences of the expanding spark channel were obtained by using the high-speed camera (Phantom v710, 6.8×10^5 fps). The spark discharge is accompanied by a shock wave generation. The shock wave pressure was measured by a fiber optic probe hydrophone (FOPH 2000). The hydrophone tip was positioned at the distance of 23 mm. Temporal voltage and current waveforms were measured by a voltage and current probes (PVM-1 2000:1, North Star Research Co., and model 4997, Pearson). The measured signals were recorded by an oscilloscope (Tektronix MD04054C).

3. Spark expansion model

Before embarking on a mathematical model, we need to clarify the physical nature of underwater spark. An application of a fast rise-time, high-voltage pulse to electrodes results in the formation of quickly growing streamer from one electrode (needle anode in our case). When the streamer reaches the opposite electrode, an electrical breakdown occurs and an electric spark is formed. In our approach we consider the spark channel as a cavity filled with uniform plasma. A number of experimental observations reveal that the vapor layer separating the spark plasma from the channel wall is extremely thin, and can be neglected [11, 12]. Due to the fact that the typical electrode gap in our experiments (0.75–0.8 mm) is comparable to the diameter of streamer (0.7 mm) before the breakdown moment, it is possible to consider the shape of the channel as a spherical with a time-varying radius *r*. A fast energy deposition into the channel leads to plasma heating and explosive channel expansion with a simultaneous gradual plasma decay. It is difficult to define precise time of plasma decay. However, the underwater spark observation period depends on a camera exposure and exceeds the period of electrical energy deposition at least by more than one order of magnitude [12, 13]. For our purposes we will limit the time range of our calculation to the value comparable to the period of electrical energy deposition (~30 µs).

Let us assume that electrical energy delivered to the plasma channel through Joule heating is divided between the internal energy of plasma–vapor mixture inside the channel, and the mechanical work done by expanding channel. Neglecting heat losses and losses due to light emission, the energy balance equation can be written as [14]:

$$\frac{d}{dt}\frac{pV}{\gamma-1}+p\frac{dV}{dt}=P_j, \tag{1}$$

where p is a pressure inside the spark, $\gamma=1.2$ is the ratio of specific heats, P_j represents Joule heating of the spark plasma, and V is volume of spark channel, which for spherical approximation is expressed as

$$V(t)=\frac{4}{3}\pi r^3(t). \tag{2}$$

For comparison with experiments, we need to find radius r and its derivatives as a function of time. The liquid compressibility was neglected in our calculations. Two mathematical expressions were examined. Naugolnych and Roy obtained equation (NRE) for the pressure p on the surface of sphere expanding in the liquid [14]:

$$p - p_0 = \rho_0 \left(\frac{3}{2}\dot{r}^2 + r\ddot{r}\right), \tag{3}$$

where ρ_0 is a liquid density; the dots denote derivatives with respect to time. Braginskii deduced expression (BE) for pressure on a spark surfaces in gas:

$$p = K\rho_0 \dot{r}^2, \tag{4}$$

where $K \approx 0.9$ is the coefficient of resistance. The gas density is replaced by liquid density ρ_0 for our aims. The applicability of this formula for the liquid will be examined in present study. Substituting successively (3) and (4) in (1) and rearranging, (1) becomes:

for NRE

$$\frac{4}{3}\pi r^3 \rho_0 (3\dot{r}\ddot{r} + \dot{r}\ddot{r} + r\dddot{r}) + 8\rho_0 \pi r^2 \left(\frac{3}{2}\dot{r}^2 + r\ddot{r}\right) = P_j(t) \tag{5}$$

and for BE

$$\frac{4}{3}\pi K \rho_0 \frac{1}{\gamma - 1}\left[2\dot{r}\ddot{r}r^2 + r^2\dot{r}^3\big(3 + 3(\gamma - 1)\big)\right] = P_j(t) \tag{6}$$

Equations (5) and (6) will be used to numerically evaluate the radius of the expanding spark and the expansion velocity. The results of these simulations will be compared with the experimental data.

Engel at al. deduced a new equation for the spark channel radius [15]. They consider a special case, when the ratio of specific heats $\gamma = 2$. Substituting BE (4) into the balance equation (1) after simplifications they derived

$$r(t) = \left[3\int_0^t \sqrt{\int_0^u \frac{P_j(v)}{\pi^2 K \rho_0} dv + \dot{r}^2(0)}\ du + r^3(0)\right]^{\frac{1}{3}} \tag{7}$$

Equation (7) will be also compared with experiment.

During the initial stage of its expansion, the plasma channel radiates an intense shock wave propagating into surroundings at approximately speed of sound $c_0 \approx 1.5$ km/s. Substituting calculated radius r in the acoustic approximation for a radiated wave [14]

$$p_w - p_0 = \frac{\rho_0}{4\pi d}\frac{\partial^2}{\partial t^2} V\left(t - \frac{r}{c_0}\right) \tag{8}$$

we get pressure in a spherical compression wave p_w propagating at a distance d from the spark.

The calculations were performed for two cases. In the first case, the power function $P_j(t) = u(t)i(t)$ was calculated from measured $u(t)$ and $i(t)$. In the second case, $P_j(t)$ was determined by solving of a differential equation describing RLC circuit:

$$\frac{d^2 i}{dt^2} + \frac{R_p + R_s}{L_c}\frac{di}{dt} + \frac{1}{L_p C_p} i = 0 \tag{9}$$

Here R_p and R_s were power supply and spark resistances, L_p was power supply inductance, C_p was capacitance of capacitor bank.

4. Numerical and experimental results

To set up the initial conditions for numerical solution of the equations (5), (6), and (8), it was assumed that at time $t = 0$ the plasma bubble was spherically shaped with initial diameter equal to the electrode gap of 0.8 mm. The measured electrical characteristics (voltage and current) of a typical discharge are shown in Fig. 2. The fundamental difference between measured and simulated voltage and current waveforms for the calculation of equations (5), (6) and (8) lies in different characterization of the spark channel resistance, which is a function depending on the plasma temperature and spark channel radius. In the case of measured voltage and current, the resistance function is determined by it and we just calculated $P_j(t) = u(t)i(t)$. The mathematical description of time dependent resistance R_s is very complicated. Therefore, a constant value of a spark channel resistance R_s was used for simulation. Calculated electrical characteristics are shown in Fig. 2.

Spark-radius time development observed directly by the high-speed camera are plotted together with calculated theoretical variations of the spark channel radius (Fig. 3). The theoretical variations have been computed using the three different expansion models (5),(6), and (8). BE (6) shows a good agreement with experiment. However, it is not perfect; discrepancy between the curve calculated using BE with the experimental power $P_j(t)$ is 0.36 mm at 10 µs from the discharge initiation. There is poor agreement between experiment and theoretical results given by NRE (5). Engel's (8) assumption about specific heat ratio $\gamma = 2$ does not seem to be suitable in this case, since it gives incorrect results. It is excluded from further considerations. Obviously, the simulations using experimentally measured voltage and current reveal better agreement with experiment than simulations using calculated values determined by eq. (9) (constant spark resistance).

The Fig. 4 depicts time dependence of spark channel expansion velocity determined either experimentally (black line) or calculated from the models (5) and (6) (color lines). As the plasma in the spark channel is not homogeneous and reveals a special time changing morphology perpendicular to the spark axis [13], the data points representing velocity of spark channel expansion do not lie on a smooth curve. Here again, BE (6) shows the best agreement with experiment.

Transient pressure waveforms measured by the optic hydrophone at the distance of 23 mm are presented in the Fig. 5. The black solid line represents experimental data recorded by the hydrophone, while the red and green lines show the simulation results derived using BE (6) and NRE (5). The amplitude of measured shock waves reached nearly 60 MPa. The signal measured by hydrophone was very weak in the case of 14 kV charging voltage and the temporal pressure waveforms were very noisy. Therefore, the calculated and measured pressure waveforms were significantly different. Nevertheless, the amplitude of shock wave of 58 MPa is correctly predicted by NRE (5); it was 45 MPa when calculated from measured voltage and current.

Acknowledgement

This work was performed under auspices and with the support of the Grant Agency of the Czech Republic (contract 18-12386S) and of the Ministry of Education, Youth, and Sports of the Czech Republic (INTER-EXCELLENCE/Inter-transfer contract LTT17015).

5. References

[1] P. Lukes *et al.*, Shock Waves, 24, 51 (2014)

[2] K. Lee *et al.*, Journal of Applied Physics, 121, 243302 (2017).

[3] S. Kumar *et al.*, Process. Technol. 209(8), 3675 (2009).

[4] S. Mujumdar *et al.*, Journal of Manufacturing Science And Engineering-Transactions of The Asme, 136, 031011 (2014)

[5] I. Timoshkin *et al.*, J. Phys. D: Appl. Phys., 39, 4808 (2006).

[6] J. A. Cook, *et al.*, Acoust. Soc. Am., 101(4), 1908 (1920)

[7] X. Lu *et al.*, J. Appl. Phys., 91, 24 (2002)

[8] K. Vokurka, *et al.*, Exp. Therm. Fluid Sci., 51, 84 (2013).

[9] Y. Huang *et al.*, Journal of Physics D: Applied Physics, 47(25), 255204 (2014)

[10] K. Chung *et al.*, Curr. Appl. Phys., 15, 977 (2015)

[11] V. Stelmashuk, IEEE Transactions on Plasma Science 42, 2626 (2014)

[12] V. Stelmashuk, Journal of Physics D-Applied Physics, 47, 495204 (2014)

[13] V. Stelmashuk, Physics of Plasma, 21, 010703 (2014)

[14] K. A. Naugol'nykh, N. A. Roy, Moscow: Nauka translation: Foreign Technology Division, Wright-Patterson AFB, OH, (1974)

[15] T. G. Engel, *et al.*, IEEE Trans. Plasma Sci., 17, 323 (1989)

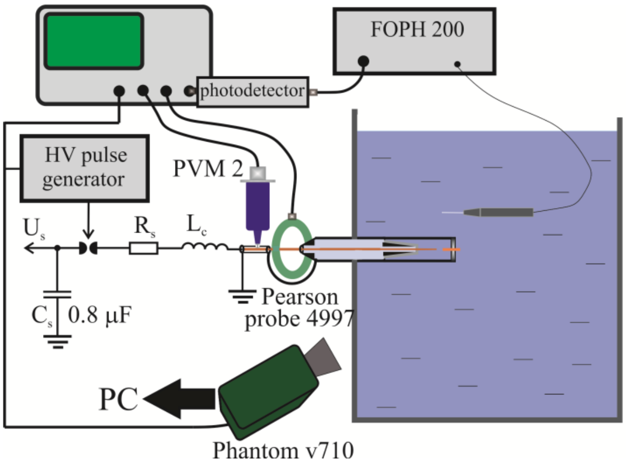

Fig. 1. Experimental setup

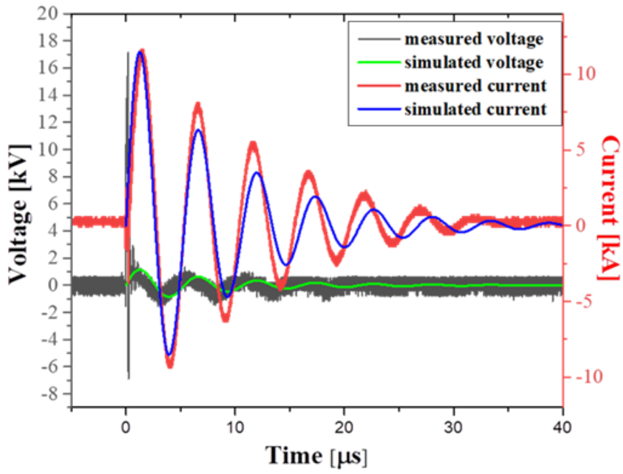

Fig. 2. The temporal voltage and current waveforms measured and calculated for 14 kV charging voltage.

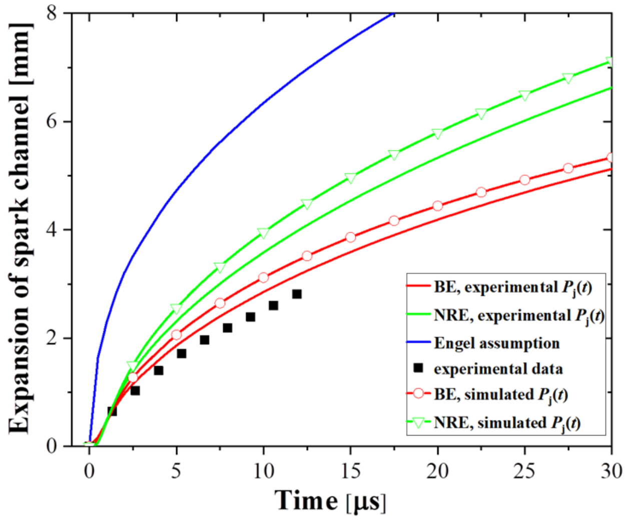

Fig. 3. Time dependence of spark radius determined either experimentally or calculated.

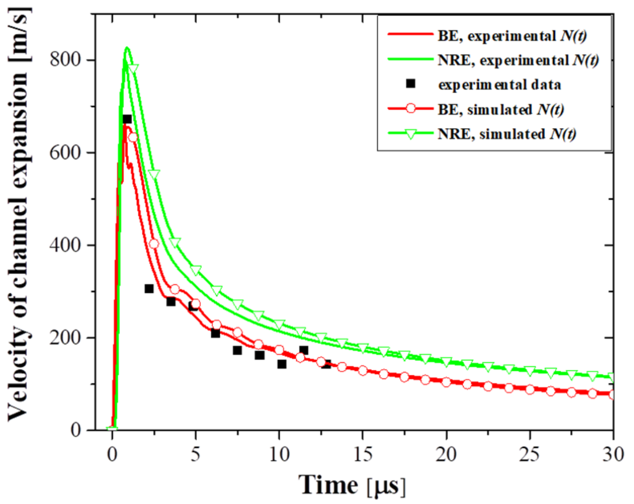

Fig. 4. Time dependence of spark channel expansion velocity determined either experimentally or calculated.

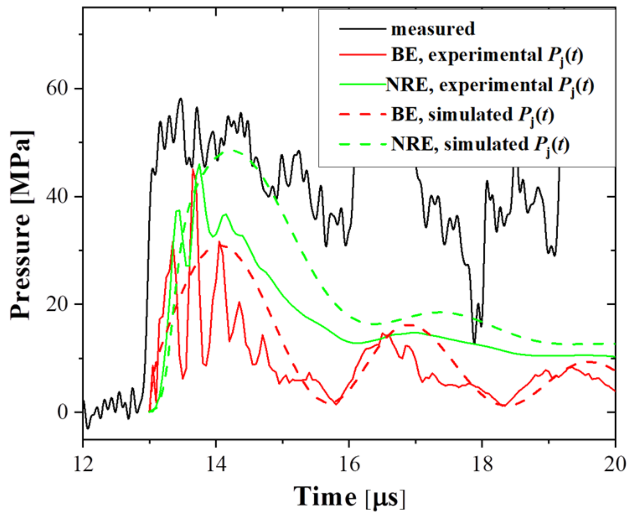

Fig. 5. Pressure waveforms at 23 mm distance from the spark determined either experimentally or calculated.